ACS OMEGA

http://pubs.acs.org/journal/acsodf

Article

Structural Analysis of Cu^{+} and Cu^{2+} Ions in Zeolite as a Nanoreactor with Antibacterial Applications

J. Flores-Valenzuela, J. E. Leal-Perez, J. L. Almaral-Sanchez, A. Hurtado-Macias, A. Borquez-Mendivil, R. A. Vargas-Ortiz, B. A. Garcia-Grajeda, S. A. Duran-Perez, and Manuel Cortez-Valadez*

Cite This: *ACS Omega* 2023, 8, 30563−30568

Read Online

ACCESS | Metrics & More | Article Recommendations

ABSTRACT: In this work, we report the structural analysis of Cu^{+} and Cu^{2+} ions in zeolite as a nanoreactor with antibacterial applications. A simple one-step process was implemented to obtain Cu ions in zeolite A (ZA4) by controlling the temperature in the solutions to guarantee the ions' stability. Samples were characterized by scanning electron microscopy, energy-dispersive X-ray spectroscopy, and Fourier transform infrared (FT-IR) spectroscopy, showing the characteristic zeolite elements as well as the characteristic bands with slight modifications in the chemical environment of the zeolite nanoreactor attributed to Cu ions by FT-IR spectroscopy. In addition, a shift of the characteristic peaks of ZA4 in X-ray diffraction was observed as well as a decrease in relative peak intensity. On the other hand, the antibacterial activity of Cu ions in the zeolite nanoreactor was evaluated.

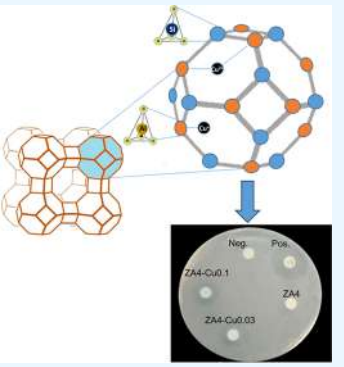

INTRODUCTION

Compared to natural zeolites, synthetic zeolites like A, X, ZSM-5, Y, P, and Na-P1 offer significant benefits due to their wider range of industrial applications. These include serving as cation exchangers, catalytic supports, selective adsorbents, and catalysts.[1−6] Due to their ability to facilitate chemical reactions in a controlled environment, zeolites fulfill the criteria to be classified as nanoreactors.[7,8] Moreover, the zeolite nanoreactor has the potential to generate a distinct and exclusive chemical environment by isolating compounds and influencing the reaction within the nanoreactor.[9] It can also be utilized to facilitate the creation of uniformly sized nanoparticles and prevent undesirable nanoparticles from sintering.[10] Zeolite has oxide-reduction capacity, which can produce Cu^{2+}, Cu^{+} and metallic Cu,[11,12] including clusters of Cu^{3+}.[13] Studies have been carried out on the ion exchange of Cu^{2+} in zeolites ZSM-5, Y, CHA, X, RTH, and LTA[14−23] and Cu^{+} has been studied in ZSM-5, CHA, and BEA[24−26] independently. A recent investigation of copper mono- and polystructures obtained in a ZSM-5 zeolite has revealed how the copper species interact with the zeolite, as well as precisely observing their positions within the zeolite structure.[27] For ZA4, there are four active sites for Cu^{2+}: SII, which is in the center of a six-ring face; SII′, located in the center of the sodalite, SII*, in the large cage; and SIII, in the D4R.[28] Moreover, studies have revealed that the redistribution in electron density modifies the distribution of charge in the Al−O bonds when the coordination of metal cations occurs in cation exchange sites in zeolites.[29] The selectivity of ion exchange generally increases as the charge and size of the exchanger ion increase.[30] Additionally, zeolites have demonstrated antibacterial properties, such as natural zeolite tuffs that contain Cu^{2+}, Zn^{2+}, or Ni^{2+}, and have been found to be highly effective against *Escherichia coli* and *Staphylococcus aureus*.[31] In experiments involving zeolite X and A with different Al/Si ratios and which were ion-exchanged with Ag^{+}, Zn^{2+}, and Cu^{2+}, it was discovered that Ag^{+}-ion-loaded zeolites exhibited the most significant antibacterial activity compared to other metal-ion-embedded zeolites.[32] Another study reports that the Cu^{2+}-ZnO-modified 13X zeolite has excellent antibacterial activity against *E. coli* and *S. aureus*.[33] Infections caused by bacteria like *E. coli* and *S. aureus* are the main causes of bacteremia and healthcare-associated infections (HAIs). Also, it is getting harder to treat infections because some bacteria have become stronger than others. Therefore, research on zeolites as a means to reduce antibacterial activity has revealed a high potential due to their large surface area and capacity to exchange metal cations, which have been extensively demonstrated for the elimination of these microorganisms, as shown in other investigations.[34−37] However, no published work has been found on Cu^{+} or Cu^{2+} ion analysis in ZA4 on structural and antimicrobial activity simultaneously.

Received: June 1, 2023
Accepted: July 27, 2023
Published: August 8, 2023

For this reason, we are interested in understanding if the addition of Cu ions to Z4A confers a potential antimicrobial agent. At present, only previous works on the alteration of the crystal structure of Z4A, attributed to the presence of Cu^{2+} ions,[38] have been found; however, they only studied the adsorption and removal of Cu(II). The purpose of this study was to determine the impact of Cu^{+} and Cu^{2+} ions in ZA4 and their effect on structural and antibacterial activity. The samples were analyzed by scanning electron microscopy-energy dispersive X-ray spectroscopy (SEM-EDS) to show the morphology and chemical composition of the samples, Fourier transform infrared (FT-IR) spectroscopy to identify changes in the chemical environment of the molecular structure of zeolite, and X-ray diffraction (XRD) to analyze changes in the crystal structure of the zeolite that vacancies or atomic substitutions can cause.

EXPERIMENTAL SECTION

Materials. Synthetic zeolite 4A (ZA4, Sigma-Aldrich), $CuSO_4{\cdot}5H_2O$ (99.5%, Sigma-Aldrich), deionized water, Gram-positive bacteria *S. aureus* (ATCC BAA-1026), and *Enterococcus faecalis* (ATCC 29212).

Methods. *Cu Ion Exchange.* 10 g of Z4A in 25 mL of deionized water was prepared for 24 h by hydration. Independently, 100 mL solutions of $CuSO_4$ for two solutions with 0.03 M (Z4A-Cu0.03) and 0.1 M (Z4A-Cu0.1) were elaborated. Subsequently, the $CuSO_4$ and hydrated zeolite solutions were placed independently in a thermal bath until obtaining a constant at 50 °C. Then, under the same temperature conditions, each $CuSO_4$ solution was added to the hydrated zeolite and maintained under magnetic stirring for 25 min to form Z4A-Cu0.03 and Z4A-Cu0.1. The solution was filtered and washed three times with deionized water to remove the remaining ions. Subsequently, drying was carried out at room temperature (30 °C in summer) to preserve the stability of the Cu ions.

Antibacterial Activity Test. The antibacterial activity of Z4A, Z4A-Cu0.03, and Z4A-Cu0.1 was tested against the Gram-positive bacteria *S. aureus* (ATCC BAA-1026) and *E. faecalis* (ATCC 29212). The bacteria were pre-grown on Luria Bertani (LB) medium overnight at 37 °C to obtain the cultures in the log phase of growth. The bacteria were diluted to 10^6 CFU using phosphate-buffered saline (PBS) and plated on Mueller−Hinton agar plates. 6 mm diameter Whatman filter paper disk were impregnated with the different materials at a concentration of 0.1 g/mL (Ertapenem/10 μg BIORAD was used as a positive control for *S. aureus,*[39] and fosfomycin/50 μg OXOID for *E. faecalis*[40] a filter paper disk with PBS only was used as a negative control), following the disk diffusion Kirby−Bauer method. Mueller−Hinton plates were incubated for 24 h at 37 °C.[41] All treatments were carried out in triplicate. The normal distribution of data was confirmed by the Shapiro−Wilk test, and the group means were compared using a one-way analysis of variance (ANOVA) and Tukey's test. The data were shown as the mean ± standard deviation (SD). The results were plotted on GraphPad Prism version 9.0. Differences between the variants were considered significant when $P < 0.05$.

Characterizations. A Hitachi SU3500 scanning electron microscope was used to determine surface changes and chemical composition (MEB-EDS). A Bruker AXS D8 forward diffractometer operated at 35 kV and 25 mA was used to determine the zeolite crystal structure (XRD). A Bruker-Alpha tensor spectrophotometer was used to determine the molecular structure of the zeolite (FT-IR).

RESULTS AND DISCUSSION

Figure 1 shows (a) SEM and (b) EDS analyses of Z4A, Z4A-Cu0.03, and Z4A-Cu0.1. In (a), a change in the surface of Z4A

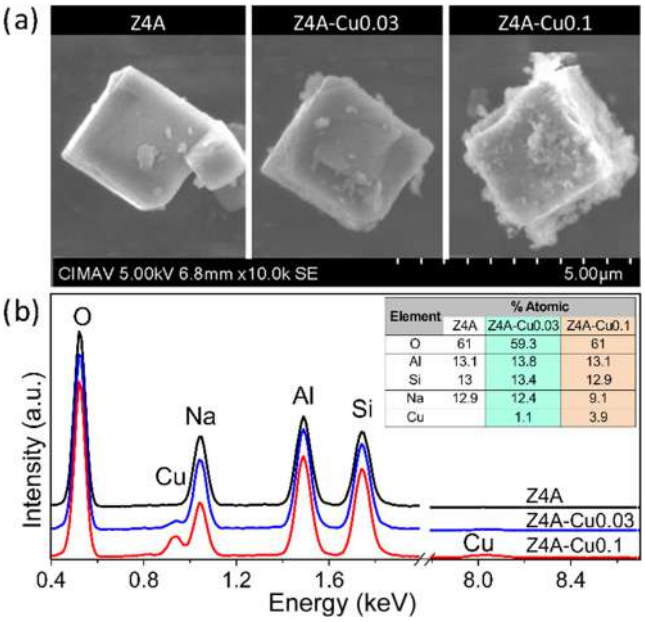

Figure 1. (a) SEM and (b) EDS analysis of Z4A, Z4A-Cu0.03, and Z4A-Cu0.1.

is observed with increasing Cu concentration regarding Z4A; this was caused by the chemical attack of the Cu solution. In (b), for Z4A, characteristic elements O, Na, Al, and Si with a 1:1:1 ratio (Na/Si/Al) are observed.

On the other hand, for Z4A-Cu0.03 and Z4A-Cu0.1, it is also observed that Cu at 0.93 keV has an evident increase related to its molar ratio (search for information about the ions in this region), conserving the 1:1:1 ratio (Na:Si:Al), which may indicate that the ionic exchange was performed in a satisfactory condition without excess Cu, which could cause agglomeration or particle formation.

Figure 2 shows the FT-IR spectra of Z4A, Z4A-Cu0.03, and Z4A-Cu0.1. Figure 2a shows the band at 1000 cm^{-1}, corresponding to the Si−O and Al−O asymmetric stretching vibration bonds (a characteristic region of the LTA zeolite). The peak at 666 cm^{-1} represents the Si−O−Al asymmetric stretching vibrational bond. The band at 554 cm^{-1} corresponds to the Si−O−Si and O−Si−O symmetrical stretching vibration bonds, attributed to the secondary structure (D4R); the bands at 1656 and 3436 cm^{-1} are assigned to the −OH vibrational stretching mode bonds of the water adsorbed on the zeolite.[8,42,43] Similarly, in all spectra. Figure 2b shows the 666 cm^{-1} regions; in each spectrum (Z4A-Cu0.03 and Z4A-Cu0.1 regarding Z4A), novel bands can be observed in the range 675−780 cm^{-1}. Moreover, an evident shift was observed in the copper samples regarding the 666 cm^{-1} band, which can be attributed to a disturbance in the chemical environment of Z4A due to the presence of ionic copper because this region is very sensitive to the changes associated with the interaction of Na^{+} and the Si−O−Al bonds. Therefore, an alteration in its molecular structure can lead to new interactions or band

https://doi.org/10.1021/acsomega.3c03869
ACS Omega 2023, 8, 30563−30568

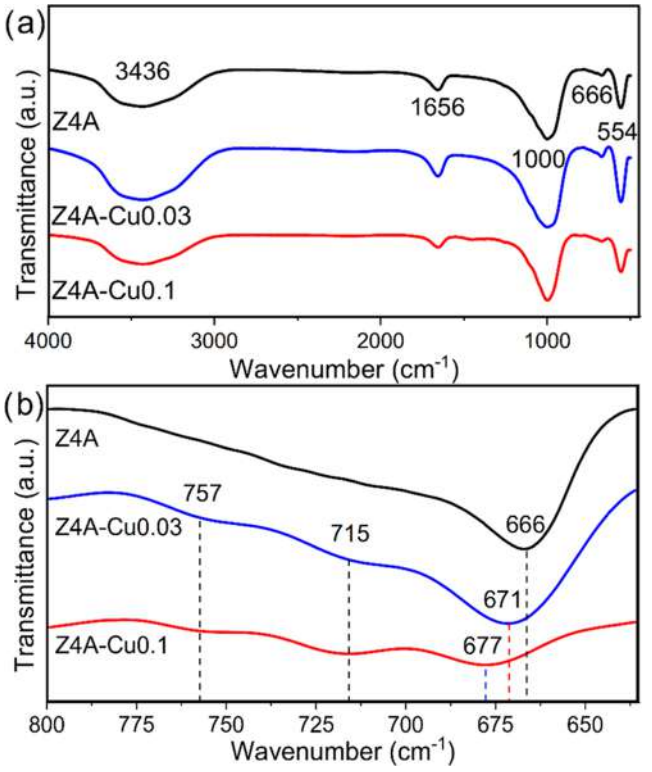

Figure 2. (a) FT-IR spectra and (b) approach in the 800−625 cm^{-1} region of Z4A, Z4A-Cu0.03, and Z4A-Cu0.1.

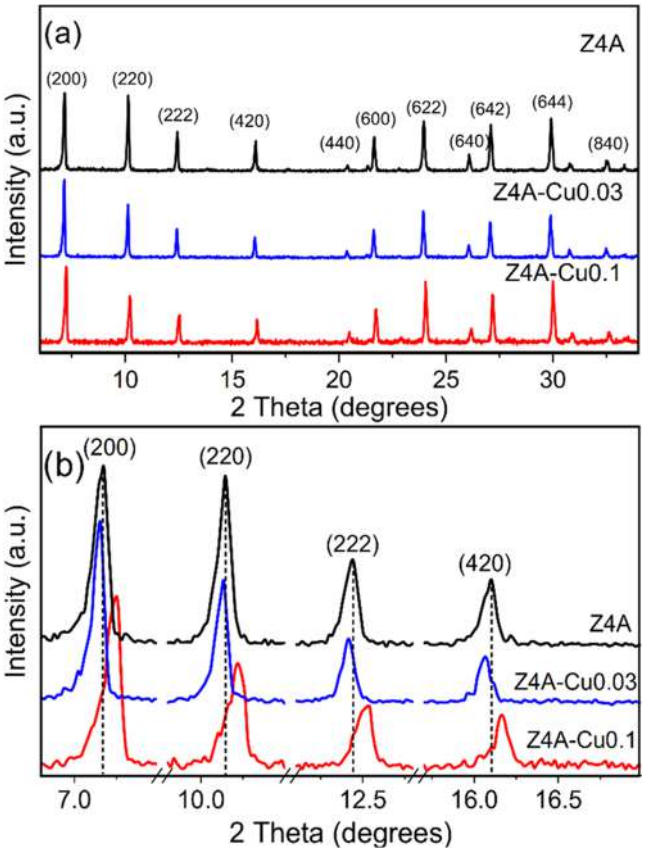

Figure 3. (a) X-ray diffraction and (b) approach to the highest peaks of Z4A, Z4A-Cu0.03, and Z4A-Cu0.1.

formation. However, the FT-IR region around 667 cm^{-1} has not been studied, and only an effect of similar behavior was found in the range close to 1000 cm^{-1}, by the formation of CuO nanoparticles and copper polylsilicates in zeolite Y[44] and LTA.[45]

Figure 3 shows X-ray diffraction of Z4A, Z4A-Cu0.03, and Z4A-Cu0.1. Figure 3a shows the characteristic XRD patterns of Z4A, indexed by JCP2 01-073-2340, without any evidence of metallic particles or copper oxides. Figure 3b shows an enlargement of normalized X-ray diffraction peaks corresponding to peaks (200), (220), (222), and (420), where the behavior of Z4A is compared with Z4A-Cu0.03 and Z4A-Cu0.1. For Z4A-Cu0.1, there was a reduction in the relative intensity of peaks (220), (222), and (420) regarding Z4A and a shift toward higher angles in peaks (200), (220), (222), and (420), which causes stress in the crystalline structure of the zeolite.[29] This could be produced by substituting one atom for another with a smaller radius, according to Bragg's law, which indicates that the interplanar distance (d) is inversely proportional to the variation in degrees (2θ) and could be attributed to the substitution of Na^+ (r = 95 pm) by Cu^{2+} (r = 72 pm).[46] This may imply that, as the concentration of the Cu ion increases, the ion exchange reaction becomes more selective toward Cu^{2+} ions, which can be placed noncoplanar by substituting one Cu atom for two Na.[38,47] For Z4A-Cu0.03 M, the relative intensity decreases in the (220), (222), and (420) peaks regarding Z4A, which can be attributed to the incorporation of Cu in Z4A. It can be observed that there is a displacement toward smaller angles in (200), (220), (222), and (420) peaks, which caused compression in the crystalline structure of the zeolite and is not an expected behavior if the incorporation of Cu were by Cu^{2+} ions. Additionally, we suppose that this effect is due to the incorporation of Cu^+, which can be accommodated in a coplanar way by replacing a Cu atom with one of Na because the Na^+ ion (r = 95 pm) when performing ion exchange with the Cu, which is estimated to be Cu^+ (r = 96 pm)[48] because the ionic radii of these are very similar. Analogous results have been reported for mono copper species identified as Cu^{2+}, which demonstrate a direct interaction between the large cavity and the single 6-atom rings of zeolite.[27]

Figure 4 shows the diameter in mm of the bacterial growth inhibition zones of Z4A, Z4A-Cu0.03, and Z4A-Cu0.1 against Gram-positive bacteria *S. aureus* and *E. faecalis*. For Z4A, no bacterial inhibition halo is observed, as in the cases of Z4A-Cu0.03 and Z4A0.1. Figure 5 shows a graph of antibacterial activity; the results show a significant difference in bactericidal

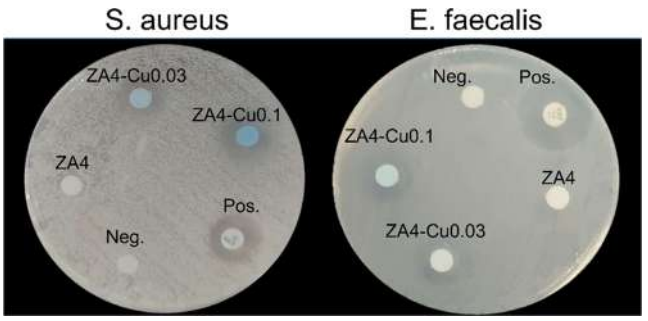

Figure 4. Diameter of the bacterial growth inhibition zones of Z4A, Z4A-Cu0.03, and Z4A-Cu0.1 against Gram-positive bacteria *S. aureus* and *E. faecalis*.

https://doi.org/10.1021/acsomega.3c03869
ACS Omega 2023, 8, 30563−30568

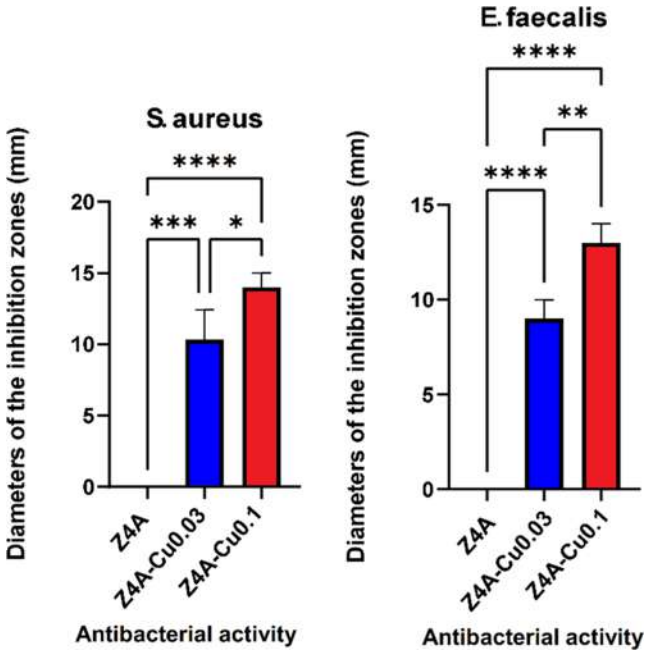

Figure 5. Graph of the antibacterial activity of Z4A, Z4A-Cu0.03, and Z4A-Cu0.1 against Gram-positive bacteria (left) *S. aureus* and (right) *E. faecalis*.

activity compared between Z4A-Cu0.03 and Z4A-Cu0.1, as well as no inhibition for Z4A. Table 1 shows the percentage inhibition of ZA4, ZA4-Cu0.03, and ZA4-Cu0.1 regarding the positive control for each of the bacterial strains tested. Comparing the effect of the materials versus the positive control on *S. aureus* growth, percent inhibition values of 67.4% and 91.3% for Z4A-Cu0.03 and Z4A-Cu0.1, respectively, show the bactericidal potential of the materials. Although in *E. faecalis*, the percentages of inhibition were lower compared to those observed for *S. aureus* (44.3% and 63.9% for Z4A-Cu0.03 and Z4A-Cu0.1, respectively), it is evident that there is a growth inhibitory effect on this bacterium.

According to the antibacterial test results, the Z4A-Cu0.03 and Z4A-Cu0.1 materials affect *S. aureus* and *E. faecalis* in vitro; in both cases, the antibiogram test showed a growth inhibition zone. The results confirm the susceptibility of these strains to the materials, consistent with that reported in other studies.[49,50] In addition, because the diameter of the inhibition halo is bigger invZ4ACu0.1 compared to Z4ACu0.03 for both (*S. aureus* and *E. faecalis*), XRD analysis allows us to elucidate that Z4ACu0.1 has been exchanged with Cu^{2+} ions and that Z4ACu0.03 has been exchanged with Cu^{+}. Our results suggest that the inhibitory effect has a behavior dependent on the charge value of the Cu ion as well as on the copper concentration. The results of examining bacteria in the laboratory reveal a thorough understanding of how the pathogen and the antibacterial agent interact and how the properties of the materials are compared. This has been demonstrated in different studies.[51,52]

CONCLUSIONS

The results suggested that ion exchange for Cu^{2+} occurred at a concentration of 0.1 M, where the relative intensity of the peaks decreased and there was displacement toward greater angles than in Z4A, which caused tension in its structure, leading to noncoplanar rearrangements due to the replacement of Na^{+} (r = 95 pm) by Cu^{2+} (r = 72 pm). The ion exchange for Cu^{+} occurred at a concentration of 0.03 M, at which the relative intensity of the peaks decreased and displacement toward smaller angles (2θ) than in Z4A was observed, which caused compression in its structure, accommodating in a coplanar way, due to the replacement of Na^{+} (r = 95 pm) by Cu^{+} (r = 96 pm). Furthermore, disturbance was observed in the ZA4 chemical environment, attributed to the presence of Cu^{+} and Cu^{2+} ions, which caused novel bands in the 667 cm^{-1} FT-IR region of the zeolite. Bactericidal tests showed good antibacterial activity mainly for ZA4-Cu0.1 (ion exchange selectivity for Cu^{2+}), indicating that this material could be used as a first filter in the elimination of *S. aureus* and *E. faecalis* bacteria.

AUTHOR INFORMATION

Corresponding Author

Manuel Cortez-Valadez − *Departamento de Investigación en Física, Universidad de Sonora, Hermosillo, Sonora 83190, México;* orcid.org/0000-0003-1323-2743; Email: manuelcortez@live.com, jose.cortez@unison.mx

Authors

J. Flores-Valenzuela − *Universidad Autónoma de Sinaloa, Los Mochis, Sinaloa 81223, México*

J. E. Leal-Perez − *Universidad Autónoma de Sinaloa, Los Mochis, Sinaloa 81223, México;* orcid.org/0000-0002-6215-1109

J. L. Almaral-Sanchez − *Universidad Autónoma de Sinaloa, Los Mochis, Sinaloa 81223, México*

A. Hurtado-Macias − *Centro de Investigación en Materiales Avanzados, Chihuahua, Chihuahua 31136, México*

A. Borquez-Mendivil − *Universidad Autónoma de Sinaloa, Los Mochis, Sinaloa 81223, México*

R. A. Vargas-Ortiz − *Universidad Autónoma de Sinaloa, Los Mochis, Sinaloa 81223, México*

Table 1. Inhibition Zone Size Around Antimicrobial Agents Tested by the Kirby−Bauer Disk Diffusion Method on Mueller−Hinton Agar[a]

		zone of inhibition (mm)		inhibition (%)	
material	dosis	*S. aureus*	*E. faecalis*	*S. aureus*	*E. faecalis*
Z4A	0.1 mg/mL	no zone	no zone	0	0
Z4A-Cu0.03	0.1 mg/mL	10.3 ± 2.1	9.0 ± 1.0	67.4 ± 0.9	44.3 ± 1.1
Z4A-Cu0.1	0.1 mg/mL	14.0 ± 1.0	13.0 ± 1.0	91.3 ± 1.3	63.9 ± 0.7
positive control	Ertapenem 10 μg	15.3 ± 0.6	N.A.		
	Fosfomycin 50 μg	N.A.	20.3 ± 0.6		

[a]N.A. = not applicable.

https://doi.org/10.1021/acsomega.3c03869
ACS Omega 2023, 8, 30563−30568

B. A. Garcia-Grajeda − *Universidad Autónoma de Sinaloa, Los Mochis, Sinaloa 81223, México*

S. A. Duran-Perez − *Doctorado en Biotecnología, Facultad de Ciencias Químico Biológicas, Universidad Autónoma de Sinaloa, Culiacán Rosales, Sinaloa 80030, México;* orcid.org/0000-0002-1009-2020

Complete contact information is available at: https://pubs.acs.org/10.1021/acsomega.3c03869

Author Contributions

Material preparation and data collection was performed by J.F.-V. and J.E.L.-P. The conceptualization and writing of the original draft of the manuscript were carried out by J.F.-V., J.E.L.-P., J.L.A.-S., and M.C.-V. The antibacterial tests were carried out by S.A.D.-P. Funding acquisition, project administration, supervision, and writing−review & editing were performed by J.F.-V. and J.L.A.-S. A.H.-M., A.B.-M., R.A.V.-O., and B.A.G.-G. contributed to results analysis and commented on previous versions of the manuscript. All authors read and approved the final manuscript.

Funding

The research was supported by (A) The DGIP at the Universidad Autónoma de Sinaloa (UAS) through the PROFAPI2015/100 and PROFAPI2022/PRO_A8_027 Projects, (B) The Consejo Nacional de Ciencia y Tecnologia (CONACYT) for its support of scholarship 924109, and (C) The Centro de Investigación en Materiales Avanzados, S.C. (CIMAV) for infrastructure support

Notes

The authors declare no competing financial interest.

■ ACKNOWLEDGMENTS

The authors acknowledge the support of the DGIP of the Universidad Autónoma de Sinaloa (UAS) for the financial support through the PROFAPI2015/100 and PROFAPI2022/PRO_A8_027 Projects; the Consejo Nacional de Humanidades, Ciencia y Tecnología (CONAHCYT) for their support of scholarship 924109; and the Centro de Investigación en Materiales Avanzados, S.C. (CIMAV), for technical support of R.P. Talamantes-Soto. The author M.C.-V appreciates the support through the "Investigadores por México" CONAHCYT program.

■ REFERENCES

(1) Scott, J.; Guang, D.; Naeramitmarnsuk, K.; Thabuot, M.; Amal, R. Zeolite synthesis from coal fly ash for the removal of lead ions from aqueous solution. *J. Chem. Technol. Biotechnol.* **2002**, *77*, 63−69.

(2) Molina, A.; Poole, C. A comparative study using two methods to produce zeolites from fly ash. *Miner. Eng.* **2004**, *17*, 167−173.

(3) Zeng, R.; Umaña, J.; Querol, X.; et al. Zeolite synthesis from a high Si-Al fly ash from East China. *J. Chem. Technol. Biotechnol.* **2002**, *77*, 267−273.

(4) Lee, J. D.; Jun, J. H.; Park, N. K.; Ryu, S. O.; Lee, T. J. A study on selective oxidation of hydrogen sulfide over zeolite-NaX and -KX catalysts. *Korean J. Chem. Eng.* **2005**, *22*, 36−41.

(5) Ahmad, W.; Ahmad, I.; Yaseen, M. Desulfurization of liquid fuels by air assisted peracid oxidation system in the presence of Fe-ZSM-5 catalyst. *Korean J. Chem. Eng.* **2016**, *33*, 2530−2537.

(6) Huang, H.; Zhu, H.; Zhang, Q.; Li, C. Effect of acidic properties of hierarchical HZSM-5 on the product distribution in methanol conversion to gasoline. *Korean J. Chem. Eng.* **2019**, *36*, 210−216.

(7) Wang, L. P.; Titov, A.; McGibbon, R.; et al. Discovering chemistry with an ab initio nanoreactor. *Nat. Chem.* **2014**, *6*, 1044−1048.

(8) Leal-Perez, J. E.; et al. Synthesis of Cu2S Ultrasmall Nanoparticles in Zeolite 4A Nanoreactor. *J. Cluster Sci.* **2022**, 1−6.

(9) De Martino, M. T.; Abdelmohsen, L. K. E. A.; Rutjes, F. P. J. T.; Van Hest, J. C. M. Nanoreactors for green catalysis. *Beilstein J. Org. Chem.* **2018**, *14*, 716−733.

(10) Lee, J. H.; Bonte, W.; Corthals, S.; et al. Zeolite Nanoreactor for Investigating Sintering Effects of Cobalt-Catalyzed Fischer-Tropsch Synthesis. *Ind. Eng. Chem. Res.* **2019**, *58*, 5140−5145.

(11) Bulánek, R.; Wichterlová, B.; Sobalík, Z.; Tichý, J. Reducibility and oxidation activity of Cu ions in zeolites effect of Cu ion coordination and zeolite framework composition. *Appl. Catal., B* **2001**, *31*, 13−25.

(12) Hoang, D. L.; Dang, T. T. H.; Engeldinger, J.; et al. TPR investigations on the reducibility of Cu supported on Al 2O3, zeolite y and SAPO-5. *J. Solid State Chem.* **2011**, *184*, 1915−1923.

(13) Leal-Perez, J. E.; Flores-Valenzuela, J.; Cortez-Valadez, M.; et al. Optical properties of copper clusters in zeolite 4A with surface enhanced Raman spectroscopy applications. *Appl. Phys. A: Mater. Sci. Process.* **2022**, *128*, No. 649.

(14) Tang, X.; Zhang, R.; Yi, H.; et al. Influence mechanism of different precursors on the adsorption behavior of NOx over Cu2+ ion-exchange ZSM-5. *J. Chem. Technol. Biotechnol.* **2019**, *94*, 3356−3366.

(15) Iwamoto, M.; Furukawa, H.; Mine, Y.; et al. Copper(II) Ion-exchanged ZSM-5 zeolites as highly active catalysts for direct and continuous decomposition of nitrogen monoxide. *J. Chem. Soc., Chem. Commun.* **1986**, *1*, 1272−1273.

(16) Seo, S. M.; Lim, W. T.; Seff, K. Crystallographic verification that copper(II) coordinates to four of the oxygen atoms of zeolite 6-rings. Two single-crystal structures of fully dehydrated, largely Cu 2+-exchanged zeolite y (FAU, Si/Al = 1.56). *J. Phys. Chem. C* **2012**, *116*, 963−974.

(17) Andersen, C. W.; Bremholm, M.; Vennestrøm, P. N. R.; et al. Location of Cu2+ in CHA zeolite investigated by X-ray diffraction using the Rietveld/maximum entropy method. *IUCrJ* **2014**, *1*, 382−386.

(18) Shan, Y.; Shi, X.; Du, J.; Yu, Y.; He, H. Cu-exchanged RTH-type zeolites for NH 3 -selective catalytic reduction of NO: X: Cu distribution and hydrothermal stability. *Catal. Sci. Technol.* **2019**, *9*, 106−115.

(19) Ryu, T.; Kim, H.; Hong, S. B. Nature of active sites in Cu-LTA NH3-SCR catalysts: A comparative study with Cu-SSZ-13. *Appl. Catal., B* **2019**, *245*, 513−521.

(20) Choi, Y. L.; et al. Preparation of Na-X and Na-A zeolites from coal fly ash in a thermoelectric power plant and comparison of the adsorption characteristics for cu(Ii) with a commercial zeolite. *Appl. Chem. Eng.* **2019**, *30*, 749−756.

(21) Lu, C.; Yu, S.; Yao, T.; et al. Zeolite X/chitosan hybrid microspheres and their adsorption properties for Cu(II) ions in aqueous solutions. *J. Porous Mater.* **2015**, *22*, 1255−1263.

(22) Wu, L.; Navrotsky, A. Synthesis and thermodynamic study of transition metal ion (Mn 2+, Co 2+, Cu 2+, and Zn 2+) exchanged zeolites A and Y. *Phys. Chem. Chem. Phys* **2016**, *18*, 10116.

(23) Yao, G.; Zhang, X.; Sun, Z.; Zheng, S. High adsorption selectivity of zeolite X in the binary ionic system of Cu(II) and Zn(II). *J. Porous Mater.* **2019**, *26*, 1197−1207.

(24) Nachtigall, P.; Nachtigallová, D.; Sauer, J. Coordination Change of Cu+ Sites in ZSM-5 on Excitation in the Triplet State: Understanding of the Photoluminescence Spectra. *J. Phys. Chem. B* **2000**, *104*, 1738−1745.

(25) Solans-Monfort, X.; Branchadell, V.; Sodupe, M.; et al. Can Cu +-exchanged zeolites store molecular hydrogen? An ab-initio periodic study compared with low-temperature FTIR. *J. Phys. Chem. B* **2004**, *108*, 8278−8286.

(26) Kefirov, R.; Penkova, A.; Hadjiivanov, K.; Dzwigaj, S.; Che, M. Stabilization of Cu+ ions in BEA zeolite: Study by FTIR spectroscopy of adsorbed CO and TPR. *Microporous Mesoporous Mater.* **2008**, *116*, 180−187.

(27) Tang, X.; Ye, J.; Guo, L.; et al. Atomic Insights into the Cu Species Supported on Zeolite for Direct Oxidation of Methane to Methanol via Low-Damage HAADF-STEM. *Adv. Mater.* **2023**, *35*, No. 2208504.
(28) Anderson, M. W.; Kevan, L. Study of Cu2+ location in zeolites Na-A and K-A by electron spin resonance and electron spin echo spectroscopies. *J. Phys. Chem. A* **1987**, *91*, 1850−1856.
(29) Šponer, J. E.; Sobalík, Z.; Leszczynski, J.; Wichterlová, B. Effect of metal coordination on the charge distribution over the cation binding sites of zeolites. A combined experimental and theoretical study. *J. Phys. Chem. B* **2001**, *105*, 8285−8290.
(30) Nasef, M. M.; Ujang, Z. Introduction to Ion Exchange Processes. In *Ion Exchange Technology I: Theory and Materials*; Luqman, M., Ed.; Springer, 2012; pp 1−39.
(31) Hrenovic, J.; Milenkovic, J.; Ivankovic, T.; Rajic, N. Antibacterial activity of heavy metal-loaded natural zeolite. *J. Hazard. Mater.* **2012**, *201−202*, 260−264.
(32) Demirci, S.; Ustaoğlu, Z.; Yilmazer, G. A.; Sahin, F.; Baç, N. Antimicrobial properties of zeolite-X and zeolite-A ion-exchanged with silver, copper, and zinc against a broad range of microorganisms. *Appl. Biochem. Biotechnol.* **2014**, *172*, 1652−1662.
(33) Ma, X.; Pei, Y.; Ma, Y.; Pu, T.; Lei, Y. Antibacterial Activity of Cu2+-ZnO-modified 13X Zeolite against *E. coli* and *S. aureus*. *J. Wuhan Univ. Technol., Mater. Sci. Ed.* **2019**, *34*, 481−486.
(34) Wang, Y.; Zhang, C.; Zhang, H.; Feng, L.; Liu, L. A hybrid nano-assembly with synergistically promoting photothermal and catalytic radical activity for antibacterial therapy. *Chin. Chem. Lett.* **2022**, *33*, 4605−4609.
(35) Li, Y.; Xia, X.; Hou, W.; et al. How Effective are Metal Nanotherapeutic Platforms Against Bacterial Infections? A Comprehensive Review of Literature. *Int. J. Nanomed.* **2023**, *18*, 1109−1128.
(36) Almessiere, M. A.; Slimani, Y.; Rehman, S.; et al. Magnetic properties, anticancer and antibacterial effectiveness of sonochemically produced Ce3+/Dy3+ co-activated Mn-Zn nanospinel ferrites. *Arabian J. Chem.* **2020**, *13*, 7403−7417.
(37) Hashim, M.; Shirsath, S. E.; Meena, S.; et al. Investigation of structural, dielectric, magnetic and antibacterial activity of Cu-Cd-Ni-FeO4 nanoparticles. *J. Magn. Magn. Mater.* **2013**, *341*, 148−157.
(38) Shen, X.; Qiu, G.; Yue, C.; Guo, M.; Zhang, M. Multiple copper adsorption and regeneration by zeolite 4A synthesized from bauxite tailings. *Environ. Sci. Pollut. Res.* **2017**, *24*, 21829−21835.
(39) Gesser, R. M.; McCarroll, K. A.; Woods, G. L. Efficacy of ertapenem against methicillin-susceptible *Staphylococcus aureus* in complicated skin/skin structure infections: Results of a double-blind clinical trial versus piperacillin-tazobactam. *Int. J. Antimicrob. Agents* **2004**, *23*, 235−239.
(40) Abbott, I. J.; van Gorp, E.; van der Meijden, A.; et al. Oral fosfomycin treatment for enterococcal urinary tract infections in a dynamic in vitro model. *Antimicrob. Agents Chemother.* **2020**, *64*, No. e00342-20.
(41) Silva, V.; Oliveira, A.; Manageiro, V.; et al. Clonal diversity and antimicrobial resistance of methicillin-resistant *Staphylococcus pseudintermedius* isolated from canine pyoderma. *Microorganisms* **2021**, *9*, No. 482.
(42) Montanari, T.; Busca, G. On the mechanism of adsorption and separation of CO2 on LTA zeolites: An IR investigation. *Vib. Spectrosc.* **2008**, *46*, 45−51.
(43) Şen, S.; Bardakçi, B.; Yavuz, A. G.; Gök, A. U. Polyfuran/zeolite LTA composites and adsorption properties. *Eur. Polym. J.* **2008**, *44*, 2708−2717.
(44) Shoja Razavi, R.; Loghman-Estarki, M. R. Synthesis and Characterizations of Copper Oxide Nanoparticles Within Zeolite Y. *J. Cluster Sci.* **2012**, *23*, 1097−1106.
(45) Li, J.; Li, M.; Song, Q.; et al. Efficient recovery of Cu(II) by LTA-zeolites with hierarchical pores and their resource utilization in electrochemical denitrification: Environmentally friendly design and reutilization of waste in water. *J. Hazard. Mater.* **2020**, *394*, No. 122554.
(46) Uçar, İ.; Karabulut, B.; Paşaoğlu, H.; Büyükgüngör, O.; Bulut, A. X-ray crystal structure and Cu2+ doped EPR studies of tetraaquabis(isonicotinamide)zinc(II) and -cobalt(II) disaccharinate 1.5 hydrate single crystals. *J. Mol. Struct.* **2006**, *787*, 38−44.
(47) Göltl, F.; Sautet, P.; Hermans, I. The impact of finite temperature on the coordination of Cu cations in the zeolite SSZ-13. *Catal. Today* **2016**, *267*, 41−46.
(48) Nebolova, P.; Spirkova, J.; Perina, V.; et al. A study of the preparation and properties of copper-containing optical planar glass waveguides. *Solid State Ionics* **2001**, *141−142*, 609−615.
(49) Dealba-Montero, I.; Guajardo-Pacheco, J.; Morales-Sánchez, E.; et al. Antimicrobial Properties of Copper Nanoparticles and Amino Acid Chelated Copper Nanoparticles Produced by Using a Soya Extract. *Bioinorg. Chem. Appl.* **2017**, *2017*, No. 1064918.
(50) Kruk, T.; Szczepanowicz, K.; Stefańska, J.; Socha, R. P.; Warszyński, P. Synthesis and antimicrobial activity of monodisperse copper nanoparticles. *Colloids Surf., B* **2015**, *128*, 17−22.
(51) Lu, J.; Chen, Y.; Ding, M.; et al. A 4arm-PEG macromolecule crosslinked chitosan hydrogels as antibacterial wound dressing. *Carbohydr. Polym.* **2022**, *277*, No. 118871.
(52) Wang, Q.; Ge, L.; Wang, L.; et al. Formulation optimization and in vitro antibacterial ability investigation of azithromycin loaded FDKP microspheres dry powder inhalation. *Chin. Chem. Lett.* **2021**, *32*, 1071−1076.

https://doi.org/10.1021/acsomega.3c03869
ACS Omega 2023, 8, 30563−30568